Novel Dinuclear Ruthenium(I) and Osmium(I) complexes containing Poly(pyrazolyl)borato Ligands. *X*-Ray Crystal Structure of [{Ru[HB($C_3H_3N_2$)$_3$](CO)$_2$}$_2$]†

Margot M. de V. Steyn*
Department of Chemistry, University of South Africa, P.O. Box 392, Pretoria 0001, Republic of South Africa
Eric Singleton, Sibbele Hietkamp, and David C. Liles
Division of Processing and Chemical Manufacturing Technology, Council for Scientific and Industrial Research [CSIR], P.O. Box 395, Pretoria 0001, Republic of South Africa

Reaction of the precursors *catena*-[Ru(O_2CMe)(CO)$_2$] (**1**) and [{Os(O_2CMe)(CO)$_3$}$_2$] (**2**) with tris- and tetrakis-(pyrazolyl)borato salts yields the neutral dimers [{M[RB(pz)$_3$](CO)$_2$}$_2$] [M = Ru, R = H, (**3**); M = Ru, R = pz, (**4**); M = Os, R = pz, (**5**); M = Os, R = H, (**6**)] (pz = $C_3H_3N_2$). Compounds (**3**)—(**6**) react with chlorinated organic solvents or Br_2 to give moderate yields of monomeric [M{RB(pz)$_3$}X(CO)$_2$] (**7**)—(**10**) (X = Cl or Br). The *X*-ray structure of compound (**3**) has been determined and shows that the two tris(pyrazolyl)borato ligands co-ordinate as tridentate chelates in a *cis* staggered configuration around the dimetal core. The compound crystallizes in the monoclinic space group $P2_1/n$ with a = 12.439(2), b = 15.380(2), c = 15.571(3) Å, β = 100.85(2)°, and Z = 4. The structure has been refined to R = 0.039 and R' = 0.029. The Ru–Ru distance of 2.882(1) Å corresponds to a normal single bond. Variable-temperature n.m.r. studies revealed interconversion of co-ordinated pyrazolyl groups in solution with ruthenium dimers (**3**) and (**4**) showing greater dynamic behaviour than the osmium analogues (**5**) and (**6**).

A vast array of cyclopentadienylmetal dimers exists, whereas relatively few containing cyclopentadienyl-like poly(pyrazolyl)-borato groups are known. The lack in the case of ruthenium and osmium seems to be mainly due to the unavailability of reliable synthetic routes. To address this problem we have investigated the use of the readily available[1] carboxylato polymer *catena*-[Ru(O_2CMe)(CO)$_2$] (**1**) and dimer [{Os(O_2CMe)(CO)$_3$}$_2$] (**2**) as precursors for ruthenium(I) and osmium(I) dimers. This study forms part of investigations in which a variety of ligands has been utilized to illustrate the versatility of (**1**) and (**2**) and their acetonitrile derivatives,[1,2] [{M(O_2CMe)(CO)$_2$(NCMe)}$_2$] (M = Os or Ru), in the synthesis of dimeric complexes containing isocyanide,[3] bidentate tertiary phosphine,[4–6] bidentate diamine[7] ligands, and pyrazolate and oxypyridinate[8] bridging groups. In this paper we report the preparation and dynamic behaviour of dimeric complexes of Ru[I] and Os[I] containing unsubstituted tris- and tetrakis-(pyrazolyl)borato ligands. In order to obtain insight into the steric requirements of and the conformation imposed by the poly(pyrazolyl)borato ligands the *X*-ray crystal structural analysis of one of the complexes has been undertaken. Attempts to synthesize dimeric complexes containing tris(pyrazolyl)borato ligands with bulky 3 substituents, HB(3R-pz)$_3$ (R = t-butyl or phenyl, pz = pyrazolyl), resulted in rapid break up of the tris(pyrazolyl)-borato anions leading to mixtures of unidentified products.

Results and Discussion

Synthetic Procedures.—The reaction of complexes (**1**) and (**2**) with 2 molar equivalents of the salts K[HB(pz)$_3$] and K[B(pz)$_4$] per dimeric unit in refluxing methanol or ethanol produces crystalline products of stoicheiometry [{M[RB(pz)$_3$](CO)$_2$}$_2$] [M = Ru, R = H, (**3**); M = Ru, R = pz, (**4**); M = Os, R = pz, (**5**)]. All the products are stable to air in the solid state but decompose slowly in solution in air to give mixtures of blue and purple compounds which have, as yet, not been characterized. The ruthenium(I) complexes (**3**) and (**4**) are yellow and the osmium(I) complex (**5**) is white. The B(pz)$_4^-$ complexes (**4**) and (**5**) have very low solubilities in most organic solvents.

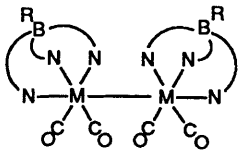

	M	R
(**3**)	Ru	H
(**4**)	Ru	pz
(**5**)	Os	pz
(**6**)	Os	H

For complex (**3**) the i.r. spectrum (see Table 1) shows characteristic bands assignable to BH and terminal CO groups [ν(B–H) 2 485; ν(CO) 2 025, 1 977, and 1 940 cm^{-1}], as well as the bands normally observed for pz groups (1 502—1 042 cm^{-1}). For compounds (**4**) and (**5**) no ν(B–H) bands are observed; a characteristic strong-weak-strong pattern [as for (**3**)] for the carbonyl stretching frequencies is observed in the terminal carbonyl regions of the spectra [ν(CO) 2 029, 1 980, and 1 944 cm^{-1} for (**4**), and 2 012, 1 965, and 1 921 cm^{-1} for (**5**)]. No bridging carbonyl species are observed in these systems using a variety of solvents, as has been observed in the i.r. spectra of the corresponding [{M(η-C_5H_5)(CO)$_2$}$_2$] (M = Fe or Ru) dimers.[9–13] On the above evidence, together with the analytical and n.m.r. spectroscopic data (see next section), dimeric structures are proposed for compounds (**3**)—(**5**) in which the RB(pz)$_3^-$ anions act as six-electron donors and the carbonyl

† Bis{dicarbonyl[tris(pyrazolyl)borato]ruthenium(I)}(*Ru–Ru*).

Supplementary data available: see Instructions for Authors, *J. Chem. Soc., Dalton Trans.*, 1990, Issue 1, pp. xix—xxii.

Table 1. Spectroscopic data for the poly(pyrazolyl)borato complexes

Complex	Infrared(cm^{-1})[a]	^1H N.m.r.(δ)[b]
(3) $[\{Ru[HB(pz)_3](CO)_2\}_2]$	2 485w, 2 025s, 1 977m, 1 940s	7.58 (6 H, d, *J* 2.2), 7.30 (6 H, br s), 6.00 (6 H, br s)
(4) $[\{Ru[B(pz)_4](CO)_2\}_2]$	2 029s, 1 980m, 1 944s	8.11 (2 H, d, *J* 2.4), 7.90 (2 H, d, *J* 1.5), 7.59 (6 H, br s), 6.63 (2 H, t, *J* 2.0), 6.17 (6 H, br s)
(5) $[\{Os[B(pz)_4](CO)_2\}_2]$	2 012s, 1 965m, 1 921s	8.72 (2 H, d, *J* 2.6), 8.14 (2 H, d, *J* 2.4), 8.03 (2 H, d, *J* 2.1), 7.92 (2 H, d, *J* 1.5), 7.13 (4 H, br s), 6.65 (2 H, t, *J* 2.0), 6.32 (2 H, t, *J* 2.2), 6.12 (4 H, br s)
(6) $[\{Os[HB(pz)_3](CO)_2\}_2]$	2 491w, 2 010s, 1 962m, 1 919s	7.88 (2 H, d, *J* 1.9), 7.77 (4 H, br s), 7.72 (2 H, d, *J* 2.7), 6.23 (2 H, t, *J* 2.2), 6.02 (4 H, br s)
(8) $[RuCl\{HB(pz)_3\}(CO)_2]$[c]	[d]2 520w, 2 074s, 2 012s	8.03 (1 H, d, *J* 2.0), 7.97 (2 H, d, *J* 2.1), 7.96 (2 H, d, *J* 2.2), 7.93 (1 H, d, *J* 2.3), 6.39 (2 H, t, *J* 2.2), 6.37 (1 H, t, 2.2)
(9) $[RuCl\{B(pz)_4\}(CO)_2]$	2 075s, 2 014s	8.27 (1 H, d, *J* 2.4), 8.16 (1 H, d, *J* 2.1), 8.09 (2 H, d, *J* 2.1), 8.06 (2 H, d, *J* 2.6), 7.97 (1 H, d, *J* 1.4), 7.51 (1 H, d, *J* 2.5), 6.70 (1 H, t, *J* 1.7), 6.44 (2 H, t, *J* 2.3), 6.38 (1 H, t, *J* 2.4)
(10) $[OsBr\{HB(pz)_3\}(CO)_2]$	[d]2 560w, 2 049s,1 979s	8.15 (1 H, d, *J* 2.0), 8.07 (2 H, d, *J* 2.1), 7.99 (1 H, *J* 2.1), 7.96 (2 H, *J* 2.4), 6.42 (2 H, t, *J* 2.3), 6.39 (1 H, t, *J* 2.3)
(11) $[OsBr\{B(pz)_4\}(CO)_2]$	2 051s, 1 982s	8.31 (1 H, d, *J* 2.3), 8.28 (1 H, d, *J* 2.0), 8.20 (2 H, d, *J* 2.0), 8.03 (2 H, d, *J* 2.6), 7.98 (1 H, d, *J* 1.1), 7.66 (1 H, d, *J* 2.7), 6.71 (1 H, t, *J* 1.9), 6.47 (2 H, t, *J* 2.4), 6.41 (1 H, t, *J* 2.4)

$^{13}C-\{^1H\}$ n.m.r. data [e]

(3)[f] 208.2 (CO), 144.7, 136.2, 106.5 (pz) **(6)**[g] 190.8 (CO), 145.1, 143.7, 135.6, 134.0, 106.4, 106.2 (pz)

[a] s = Strong, m = medium, and w = weak. In CH_2Cl_2 unless otherwise stated. [b] br = broad, s = singlet, d = doublet, and t = triplet. In $(CD_3)_2CO$ at 500 MHz and 303 K, *J* values in Hz. [c] Known compound.[16] [d] ν(BH) In Nujol. [e] At 126 MHz and 303 K. [f] In $(CD_3)_2CO$. [g] In CD_2Cl_2.

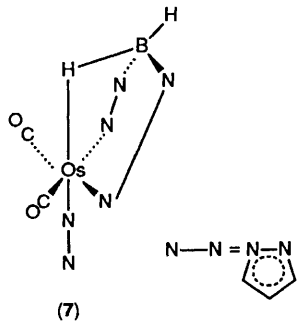

(7)

groups appear in the equatorial planes *trans* to the pyrazolyl nitrogen-donor atoms. The structure of **(3)** has been confirmed by an *X*-ray crystallographic structure determination.

Treatment of the osmium carboxylato dimer **(2)** with $K[HB(pz)_3]$ gives a yellow precipitate containing a mixture of $[\{Os[HB(pz)_3](CO)_2\}_2]$ **(6)** and a minor product. Recrystallization of the mixture produced pure **(6)** which on the basis of i.r. [ν(B–H) 2 491; ν(CO) 2 010, 1 962, and 1 919 cm^{-1}] and n.m.r. data has been assigned a dimeric structure as for **(3)**. The minor product **(7)** of this reaction could not be obtained free from **(6)** and probably results from fragmentation of the tris(pyrazolyl)borato ligand and rupture of the Os–Os bond. Multiple microanalyses of the mixture of **(6)** and **(7)** gave the same values for C, H, and N as for **(6)**, indicating that **(7)** has the same stoicheiometry as for **(6)**. The i.r. spectrum of **(7)**, obtained by subtracting the spectrum of the known compound **(6)** from the spectrum of the mixture, contains two bands of equal intensity at 2 031 and 1 955 cm^{-1}. No N–H stretching vibration is observed. The ^1H n.m.r. spectrum of **(7)** contains two different pyrazolyl resonance patterns [7.99(H, d), 7.85(H, d), 7.82(2 H, d), 7.80 (2 H, d), 6.32 (H, t), and 6.31 (2 H, t)] in the ratio 2:1 and is temperature invariant. Each pattern consists of three proton resonances observed as a triplet and a pair of doublets due to the differing environments of the two nitrogen atoms in the pyrazolyl groups. From the evidence presented here **(7)** is proposed to be an osmium(II) complex containing an agostic B–H interaction without which the complex would formally be a 16-electron system. An unsymmetrical three-centre two-electron bond formed by hydrogen bridging of one of the B–H hydrogen atoms has been observed[14,15] for complexes of $H_2B(pz)_2^-$. Unfortunately the carbonyl vibrations of the mixture obscure the region expected for Os···H–B interaction.

Reaction of complexes **(3)** and **(4)** in refluxing $CHCl_3$ or CCl_4 results in rupture of the metal–metal bond to give $[RuCl\{HB(pz)_3\}(CO)_2]$ **(8)** and $[RuCl\{B(pz)_4\}(CO)_2]$ **(9)**, respectively. The spectroscopic data for **(8)** are similar to those of the complexes $[Ru\{HB(pz)_3\}X(CO)_2]$ (X = Cl, Br, or I) prepared earlier[16] by the reaction of $RB(pz)_3^-$ and $[Ru_3(CO)_{12}]$ and subsequent treatment with halogen. A typical i.r. absorption for the B–H bond is observed in the spectrum for **(8)** [ν(B–H) 2 520 cm^{-1}]. The two strong ν(CO) bands in the i.r. spectra of **(8)** and **(9)** are similar in appearance and position to those found for the related[17] $[Ru(\eta\text{-}C_5H_5)X(CO)_2]$ complexes,

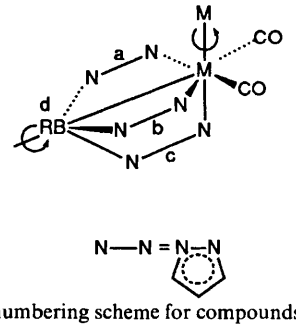

Figure 1. N.m.r. numbering scheme for compounds (3)—(6)

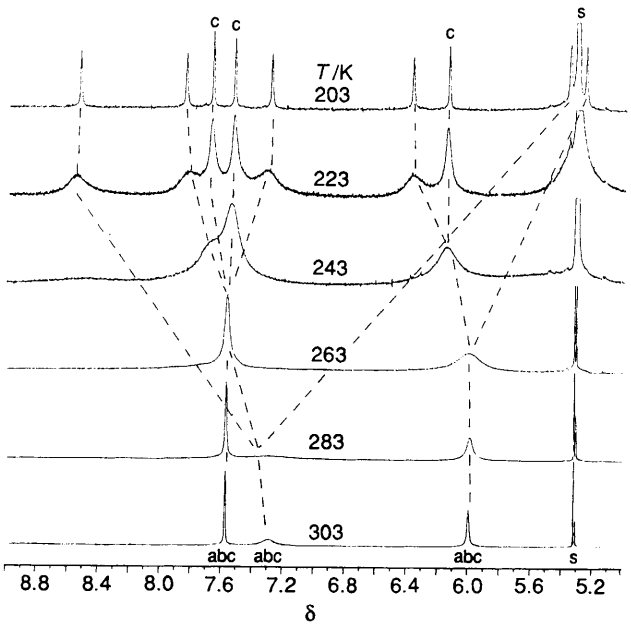

Figure 2. Proton n.m.r. spectra of complex (3) in CD_2Cl_2 at various temperatures (s represents the resonance of the solvent)

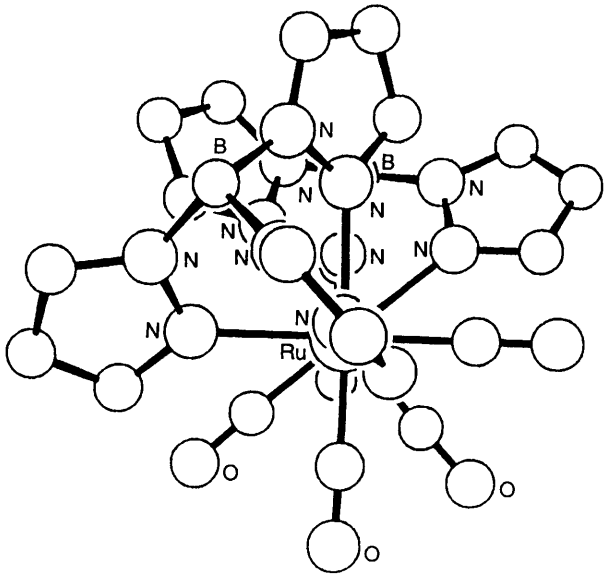

Figure 3. A projection of complex (3) down the ruthenium–ruthenium bond

suggesting the presence of two mutually *cis* carbonyl groups. The n.m.r. spectrum of complex (**8**) contains two different pyrazolyl resonance patterns in the ratio 2:1 and is temperature invariant. This is consistent with a static unsymmetrically co-ordinated tris(pyrazolyl)borato ligand. In the case of (**9**) a third pyrazolyl resonance pattern for the unco-ordinated pyrazolyl appears resulting in a 2:1:1 integration ratio for the pyrazolyl rings as expected for a non-fluxional tetrakis(pyrazolyl)borato ligand. Reaction of complexes (**6**) and (**5**) with bromine in a chloroform solution gives good yields of the compounds $[OsBr\{HB(pz)_3\}(CO)_2]$ (**10**) and $[OsBr\{B(pz)_4\}(CO)_2]$ (**11**), respectively. Both the i.r. and ^1H n.m.r. spectra closely resemble those of (**8**) and (**9**) [ν(B–H) 2 560 cm^{-1} for (**10**)].

Proton and $^{13}C-\{^1H\}$ *N.m.r Studies and Dynamic Behaviour.*—Proton and $^{13}C-\{^1H\}$ n.m.r. data are presented in Table 1. Compounds (**3**)—(**6**) display an interesting variety of stereochemical non-rigidity at different temperatures amenable to n.m.r. studies. The changes observed are all explicable in terms of the structures suggested for these compounds. The two dynamic processes occurring are internal rotation around the metal–metal bond and rotation[15] of the triangular face bridged by the $RB(pz)_3^-$ ligand about the M • • • B axis. Figure 1 illustrates these rotation processes and presents the numbering of the pyrazolyl rings used in the discussion. The changes in the dynamic behaviour of the pyrazolyl groups can be followed by monitoring the changes in the expected resonances of the three protons (*i.e.* a triplet and a pair of doublets) of the pyrazolyl rings. No BH protons are observed for (**3**) and (**6**) in their ^1H n.m.r. spectra due to broadening by the quadruple moment of the boron isotopes. The dotted lines in Figure 2 and 4—7 represent the transformations of the proton resonances from the high-temperature, at which the dynamic processes occur, to the low-temperature state (corresponding to the solid-state structure).

The ^1H n.m.r. spectrum at 303 K of the ruthenium(I) compound (**3**) shows one doublet and two broad resonances for the three protons of the pyrazolyl rings, indicating equilibration of the three pyrazolyl rings probably by non-dissociative rotation[15] of the tris(pyrazolyl)borato group around the M • • • B axis as has been observed for monomeric tris(pyrazolyl)borato transition-metal complexes (see Figure 2). At lower temperatures the resonances broaden, until at 223 K one pyrazolyl group appears as three singlets while other resonances remain diffuse. At this temperature rotation around the M • • • B axis has stopped and the observed pattern is now accounted for by a rotation around the metal–metal bond which renders equatorial pyrazole groups (rings a and b) equivalent, whilst the axial pyrazolyl group is unique. The low-temperature-limiting spectrum is reached at 203 K where both rotation around M • • • B and the metal–metal bond has stopped, showing nine sharp resonances for the protons of the three inequivalent pyrazolyl groups. A projection of the dimeric molecule down the ruthenium–ruthenium bond illustrates the different magnetic environments of the equatorial pyrazolyl groups (see Figure 3). The $^{13}C-\{^1H\}$ n.m.r. spectra at various temperatures confirm these observations.

In the case of the osmium(I) analogue (**6**) of compound (**3**) simultaneous interconversion of the pyrazolyl rings a—c does not occur at 303 K (see Figure 4). The two well resolved doublets and a triplet are invariant with temperature and represent ring c, co-ordinated axially to the metal–metal bond. The interconverting rings a and b are represented by two broad singlets and are probably equilibrated by rotation around the osmium–osmium bond, as with (**3**) at 223 K. The broad singlets disappear into the baseline at 253 K to reform at 193 K as six resonance lines representative of rings a and b. The low-temperature-limiting spectrum of (**6**) having nine resonance lines has an appearance almost identical to that of (**3**). These observations for (**6**) are supported by its $^{13}C-\{^1H\}$ n.m.r. spectra at various temperatures with the exception that the two sets of

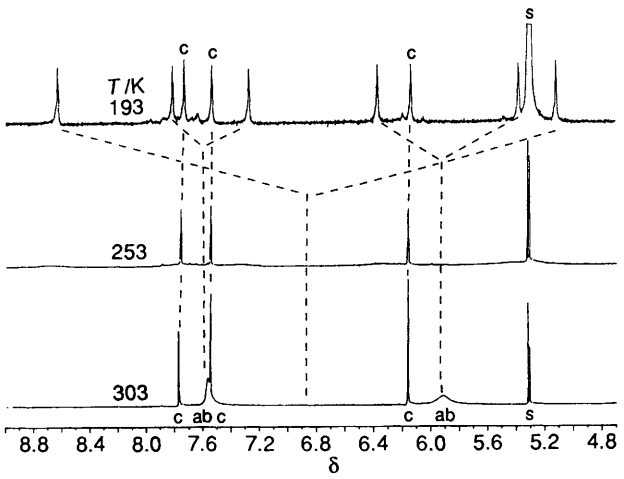

Figure 4. Proton n.m.r. spectra of complex (**6**) in CD_2Cl_2 at various temperatures (s represents the resonance of the solvent)

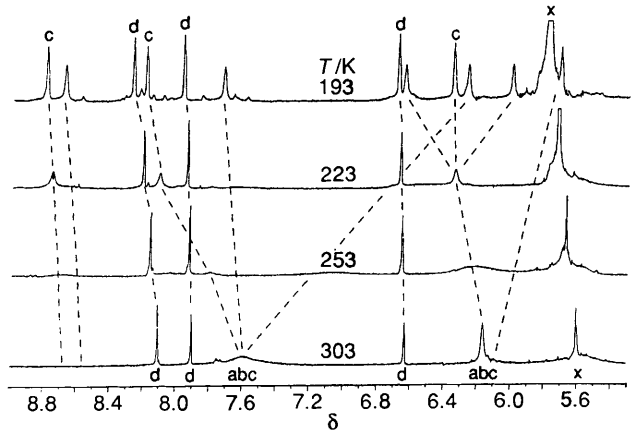

Figure 5. Proton n.m.r. spectra of complex (**4**) in $(CD_3)_2CO$ at various temperatures (x represents the resonance of an impurity)

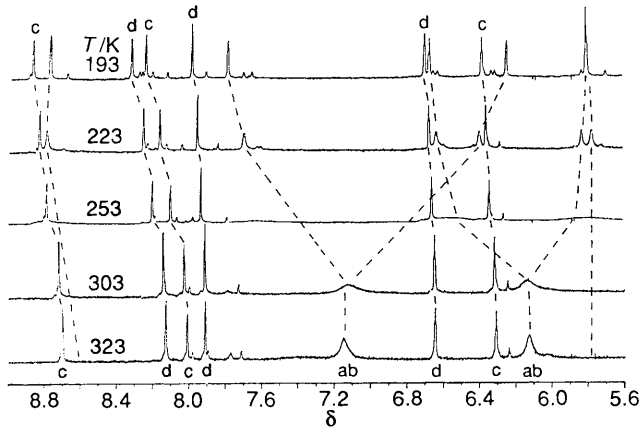

Figure 6. Proton n.m.r. spectra of complex (**5**) in $(CD_3)_2CO$ at various temperatures

pyrazolyl frequencies at 303 K are better resolved due to the smaller chemical shift difference (in Hz) of the exchanging nuclei.

The ^1H n.m.r. spectrum of the ruthenium(I) compound (**4**) (see Figure 5) shows that one pyrazolyl ring, probably the uncoordinated ring d, exhibits well resolved resonance lines between 303 and 193 K and does not interconvert with other rings. Rings a—c are observed as two broad resonances at 303 K due to rapid exchange, probably by the face-bridged rotation about M • • • B as observed for (**3**). At lower temperatures these broad

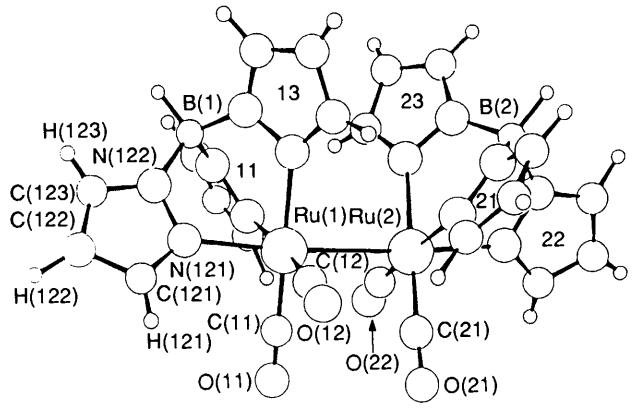

Figure 7. A perspective view of $[\{Ru[HB(pz)_3](CO)_2\}_2]$ (**3**) showing the atom numbering scheme

resonances broaden further until they start to reform at 223 K. At 193 K twelve resonances, four triplets and eight doublets, are observed indicating that all pyrazole rings are inequivalent and that both rotation about the M • • • B axis and internal rotation have ceased. The ^1H n.m.r. spectra for the osmium(I) analogue (**5**) show four well resolved doublets and two triplets from two pyrazolyl rings that are invariant with temperature and do not interconvert with other rings (see Figure 6). These resonances can probably be assigned to the free pyrazolyl ring, d, and the axially co-ordinated ring c by analogy with compounds (**4**) and (**6**). At 323 K two broad resonances are oberved for rings a and b which broaden at lower temperatures until they start to reform as six resonances at 223 K. At 193 K the resonances sharpen into eleven lines (accidental overlap of two resonances) representative of four inequivalent pyrazolyl rings. The low-temperature-limiting spectra of (**4**) and (**5**) are almost identical and the ring d protons in Figure 6 are assigned by comparison. Impurity resonances appear pronounced due to the low solubility of (**4**) and (**5**). Furthermore, the low solubility in the usual organic solvents precluded measurement of $^{13}C-\{^1H\}$ n.m.r. spectra.

Comparing the dynamic behaviour of the compounds $[\{M[HB(pz)_3](CO)_2\}_2]$ and $[\{M[B(pz)_4](CO)_2\}_2]$ (M = Ru or Os) it appears that the barrier to M • • • B rotation is lower in the case of the ruthenium(I) compounds than for their osmium(I) analogues and is probably a consequence of the weaker M–N σ bonds in the ruthenium(I) complexes. Thus, at room temperature interconversion of axial and equatorial pyrazolyl groups is not observed in the case of the osmium(I) compounds, although the equatorial pyrazolyl groups are equivalent due to rotation around the metal–metal bond.

Structure of $[\{Ru[HB(pz)_3](CO)_2\}_2]$ (**3**).—Relevant bond lengths and bond and torsion angles of compound (**3**) are given in Table 2. The molecular structure is shown in Figure 7.

The ruthenium centres in this binuclear molecule are linked by an unsupported ruthenium–ruthenium bond of length 2.882(1) Å. The diruthenium centre is flanked by two mutually *cis*-disposed tris(pyrazolyl)borato ligands. Each ruthenium has a distorted octahedral geometry in which the three 2-N nitrogen atoms of the tris(pyrazolyl)borato anion occupy two equatorial and one axial co-ordination sites. The other octahedral co-ordination positions are occupied by the other ruthenium atom and two carbon atoms from terminal carbonyls situated *trans* to the equatorial tris(pyrazolyl)borato nitrogen atoms. Octahedral angles around the Ru atom range from 80.0(1) to 98.7(1)°. The configuration of the equatorial donor atoms is staggered with respect to the donor atoms on the opposite metal atoms, with torsion angles ranging from 36.1(2)

Table 2. Relevant bond lengths (Å) and bond and torsion angles (°) for $[\{Ru[HB(pz)_3](CO)_2\}_2]$ (**3**)

Ru(1)–C(11)	1.847(5)	Ru(1)–C(12)	1.853(5)
Ru(1)–N(111)	2.174(3)	Ru(1)–N(121)	2.191(4)
Ru(1)–N(131)	2.155(4)	Ru(1)–Ru(2)	2.882(1)
B(1)–N(112)	1.550(7)	B(1)–N(122)	1.546(8)
B(1)–N(132)	1.533(7)	C(11)–O(11)	1.149(6)
C(12)–O(12)	1.138(6)	N(111)–N(112)	1.365(5)
N(121)–N(122)	1.356(5)	N(131)–N(132)	1.361(5)
Ru(2)–C(21)	1.843(5)	Ru(2)–C(22)	1.852(5)
Ru(2)–N(211)	2.177(4)	Ru(2)–N(221)	2.199(4)
Ru(2)–N(231)	2.160(3)	B(2)–N(212)	1.536(7)
B(2)–N(222)	1.543(7)	B(2)–N(232)	1.534(7)
C(21)–O(21)	1.150(6)	C(22)–O(22)	1.153(6)
N(211)–N(212)	1.365(6)	N(221)–N(222)	1.357(6)
N(231)–N(232)	1.361(6)		
C(11)–Ru(1)–C(12)	89.4(2)	C(11)–Ru(1)–N(111)	90.5(2)
C(11)–Ru(1)–N(121)	96.6(2)	C(12)–Ru(1)–N(121)	94.6(2)
N(111)–Ru(1)–N(121)	80.4(1)	C(12)–Ru(1)–N(131)	92.7(2)
N(111)–Ru(1)–N(131)	87.5(1)	N(121)–Ru(1)–N(131)	84.3(1)
C(11)–Ru(1)–Ru(2)	88.1(2)	C(12)–Ru(1)–Ru(2)	86.9(1)
N(111)–Ru(1)–Ru(2)	98.2(1)	N(121)–Ru(1)–Ru(2)	175.1(1)
N(131)–Ru(1)–Ru(2)	90.9(1)	N(112)–B(1)–N(122)	106.9(4)
N(112)–B(1)–N(132)	110.1(4)	N(122)–B(1)–N(132)	108.4(4)
Ru(1)–C(11)–O(11)	178.1(4)	Ru(1)–C(12)–O(12)	176.0(4)
Ru(1)–Ru(2)–C(21)	88.2(2)	Ru(1)–Ru(2)–C(22)	85.8(1)
C(21)–Ru(2)–C(22)	89.7(2)	Ru(1)–Ru(2)–N(211)	98.7(1)
C(21)–Ru(2)–N(211)	89.6(2)	Ru(1)–Ru(2)–N(221)	175.8(1)
C(21)–Ru(2)–N(221)	95.7(2)	C(22)–Ru(2)–N(221)	95.5(2)
N(211)–Ru(2)–N(221)	80.0(1)	Ru(1)–Ru(2)–N(231)	91.6(1)
C(22)–Ru(2)–N(231)	93.4(2)	N(211)–Ru(2)–N(231)	87.4(1)
N(221)–Ru(2)–N(231)	84.4(1)	N(212)–B(2)–N(222)	107.5(4)
N(212)–B(2)–N(232)	110.1(4)	N(222)–B(2)–N(232)	107.7(4)
Ru(2)–C(21)–O(21)	177.6(5)	Ru(2)–C(22)–O(22)	174.4(4)
Torsion angles			
N(111)–Ru(1)–Ru(2)–N(231)	52.5(2)	C(12)–Ru(1)–Ru(2)–N(211)	−41.2(2)
N(111)–Ru(1)–Ru(2)–C(22)	−41.8(2)	C(12)–Ru(1)–Ru(2)–C(21)	48.1(2)
N(131)–Ru(1)–Ru(2)–N(231)	−36.1(2)	C(11)–Ru(1)–Ru(2)–C(21)	−41.4(2)
N(131)–Ru(1)–Ru(2)–N(211)	51.5(2)	C(11)–Ru(1)–Ru(2)–C(22)	−48.4(2)

to 52.5(2)°. The tris(pyrazolyl)borato groups have local C_{3v} symmetry with H–B ··· Ru lying on the C_3 axis. Thus, the boron atoms are each tetrahedrally bonded to a hydrogen atom and three pyrazolyl groups through 1-N, fanned out in a blade-like fashion. The terminal carbonyl atoms lean slightly towards the metal–metal bond [Ru–Ru–C 87.2° (av.)], whereas the equatorial nitrogen atoms are pulled towards the boron atom [Ru–Ru–N_{eq} 94.8°(av.)]. Axial nitrogen atoms deviate only by *ca.* 5° from the Ru–Ru axis with Ru–Ru–$N_{ax.}$ angles of 175.1(1) and 175.8(1)°. Closest non-bonded contacts are between carbonyl oxygen atoms O(12) and O(22) and opposite pyrazolyl hydrogen atoms H(211) and H(111) at 2.41 and 2.39 Å, respectively. The Ru–N distances are longer for axial [2.20 Å(av.)] than for equatorial [2.17 Å(av.)] nitrogen atoms, probably as a result of the strong *trans* influence of the metal–metal bond seen previously in d^7–d^7 systems.[18,19]

The construction of a model using the parameters obtained from the *X*-ray crystal-structure determination has demonstrated the steric requirements of the four possible conformations of the molecule having terminal carbonyls, *i.e. trans* eclipsed and staggered and *cis* eclipsed and staggered forms, Rotation of the model from the *cis* staggered to the *cis* eclipsed form resulted in close approach of the 3-H atoms of the four equatorial pyrazolyl groups on opposite metal atoms. In the case of the *trans* staggered form the 3-H atoms of two of the equatorial pyrazolyl groups came into close proximity. In the *trans* eclipsed form the non-bonded repulsions between carbonyl carbon atoms and the equatorial pyrazolyl groups on opposite metal atoms seemed to render that conformation energetically less favourable. Thus, on steric considerations the *cis* staggered form reflects minimized interactions between the ligands on opposite metal atoms.

A comparison[20] between poly(pyrazolyl)borato and cyclopentadienyl ligands in dimeric rhodium(I) complexes shows a larger degree of carbonyl bridging in $[Rh_2\{HB(pz)_3\}_2(\mu\text{-}CO)_3]$ than in its unsubstituted cyclopentadienyl analogue. This trend, suggested to be consistent with the greater steric demand of the poly(pyrazolyl)borato ligand, does not apply in the case of (**3**) when compared to the solid-state structure[21] of its bridged analogue $[\{Ru(\eta\text{-}C_5H_5)(CO)_2\}_2]$. A comparison between the poly(pyrazolyl)borato[22] and cyclopentadienyl ligands[23,24] in dimeric molybdenum complexes $[\{MoL(CO)_2\}_2]$ [L = $HB(pz)_3^-$, $\eta\text{-}C_5H_5$, or $\eta\text{-}C_5Me_5$] likewise revealed very little bonding interaction of the carbonyls on each molybdenum with the remote molybdenum (average Mo≡Mo–CO angle for interacting COs 70.5°) for L = $HB(pz)_3^-$, as opposed to bridged and semibridged structures for L = C_5Me_5 and C_5H_5, respectively (average Mo≡Mo–CO angles for interacting COs 56.8 and 67.4°, respectively). A model demonstrated that a structure for (**3**) having two terminal and two bridging carbonyls is sterically impossible because of overlap of equatorial pyrazolyl rings on opposite metal atoms in the *cis* orientated poly(pyrazolyl)borato compound and close approach of the 3-H atoms of the pyrazolyl rings and the O atoms

of the terminal carbonyls in the *trans* compound. The Ru–Ru distance in complex (**3**), 2.882(1) Å, may be compared to that of 2.735(2) Å in $[\{Ru(\eta\text{-}C_5H_5)(CO)_2\}_2]$.[21] The main structural differences between (**3**) and $[\{Mo[HB(pz)_3](CO)_2\}_2]$ are the *trans* orientation of the poly(pyrazolyl)borato ligands and the non-linearity of M–M–$N_{ax.}$ in the latter case as opposed to a *cis* ligand orientation and an almost linear M–M–$N_{ax.}$ bond in (**3**). These differences together with the more acute M–M–CO angles observed for the molybdenum dimer are probably a consequence of the greater steric crowding around its dinuclear core which has a Mo=Mo distance of 2.507(1) Å. The absence of crystallographic data for $[\{Ru(\eta\text{-}C_5Me_5)(CO)_2\}_2]$ precludes further comparisons in the case of ruthenium(I) dimers.

Experimental

General Comments.—All solvents were dried and distilled prior to use under a dinitrogen atmosphere and all manipulations were routinely carried out under nitrogen using Schlenk conditions. Complexes (**1**) and (**2**) were prepared[25] from commercially available ruthenium trichloride hydrate and osmium tetraoxide, respectively, and the poly(1-pyrazolyl)borates were prepared from potassium tetrahydroborate and pyrazole according to the published[26] methods. I.r. spectra were recorded on a Bruker IFS 85 FT-IR spectrometer, ^1H and $^{13}C\text{-}\{^1H\}$ n.m.r. spectra on a Bruker WM-500 spectrometer. Elemental analyses were performed by the Microanalytical Section of the Division of Processing and Chemical Manufacturing Technology, CSIR, Pretoria.

Preparation of Compounds.—The i.r. and n.m.r. data of the new compounds are reported in Table 1.

(*a*) $[\{Ru[HB(pz)_3](CO)_2\}_2]$ (**3**). A suspension of complex (**1**) (0.50 g, 2.3 mmol) and $K[HB(pz)_3]$ (0.63 g, 2.5 mmol) in methanol (30 cm^3) was heated under reflux for 20 min during which time a yellow crystalline product separated. The mixture was cooled and filtered. Recrystallization from dichloromethane–methanol afforded the pure pale yellow product. Yield 0.50 g (0.68 mmol, 58%) (Found: C, 35.65; H, 2.50; N, 22.30. Calc. for $C_{22}H_{20}B_2N_{12}O_4Ru_2$: C, 35.65; H, 2.70; N, 22.80%).

(*b*) $[\{Ru[B(pz)_4](CO)_2\}_2]$ (**4**). A suspension of complex (**1**) (0.22 g, 1.0 mmol) and $K[B(pz)_4]$ (0.32 g, 1.0 mmol) in methanol (25 cm^3) was heated under reflux for 30 min to give a pale yellow suspension. Solvent was removed and the sparsely soluble product extracted with dichloromethane. Addition of methanol and reduction of the volume afforded the pale yellow crystalline product. Yield 0.39 g (0.45 mmol, 88%) (Found: C, 38.60; H, 2.50; N, 25.30. Calc. for $C_{28}H_{24}B_2N_{16}O_4Ru_2$: C, 38.55; H, 2.75; N, 25.70%).

(*c*) $[\{Os[B(pz)_4](CO)_2\}_2]$ (**5**). A solution of complex (**2**) (0.33 g, 0.50 mmol) and $K[B(pz)_4]$ (0.32 g, 1.0 mmol) in methanol (25 cm^3) was heated under reflux for 30 min to give a white crystalline precipitate. The mixture was cooled and the product removed by filtration. Recrystallization of the sparsely soluble solid from acetone–ethanol gave the pure product. Yield 0.28 g (0.26 mmol, 53%) (Found: C, 31.70; H, 2.15; N, 21.05. Calc. for $C_{28}H_{24}B_2N_{16}O_4Os_2$: C, 32.20; H, 2.30; N, 21.35%).

(*d*) $[\{Os[HB(pz)_3](CO)_2\}_2]$ (**6**). A solution of complex (**2**) (0.44 g, 0.66 mmol) and $K[HB(pz)_3]$ (0.37 g, 1.4 mmol) in EtOH (30 cm^3) was heated under reflux for 2 h during which time a yellow crystalline precipitate formed. The solid was separated by filtration and shown spectroscopically to contain the product and in smaller yield an unidentified product. Recrystallization from acetone–ethanol afforded only a white crystalline product. Yield 0.28 g (0.30 mmol, 46%) (Found: C, 28.55; H, 1.80; N, 17.50. Calc. for $C_{22}H_{20}B_2N_{12}O_4Os_2$: C, 28.75; H, 2.20; N, 18.30%).

(*e*) $[RuCl\{HB(pz)_3\}(CO)_2]$ (**8**). A suspension of complex (**3**) (0.52 g, 0.70 mmol) was heated under reflux in carbon tetrachloride (30 cm^3) for 12 h. Unreacted starting material was removed by filtration and solvent then removed under reduced pressure. The residue was redissolved in acetone to give a pale yellow crystalline product on addition of ethanol. Yield 0.15 g (0.37 mmol, 26%) (Found: C, 33.05; H, 2.60; Cl, 8.75; N, 20.20. Calc. for $C_{11}H_{10}BClN_6O_2Ru$: C, 32.55; H, 2.50; Cl, 8.75; N, 20.70%).

(*f*) $[RuCl\{B(pz)_4\}(CO)_2]$ (**9**). A suspension of complex (**4**) (0.44 g, 0.50 mmol) was heated under reflux in chloroform (25 cm^3) for 1.5 h. The resulting solution was filtered. Addition of ethanol to the filtrate and reduction of the volume afforded a beige crystalline product. Yield 0.18 g (0.38 mmol, 38%) (Found: C, 35.70; H, 2.50; Cl, 7.60; N, 23.15. Calc. for $C_{14}H_{12}BClN_8O_2Ru$: C, 35.65; H, 2.55; Cl, 7.50; N, 23.75%).

(*g*) $[OsBr\{HB(pz)_3\}(CO)_2]$ (**10**). A solution of complex (**6**) (0.40 g, 0.44 mmol) in chloroform (30 cm^3) was treated with a 1 mol dm^{-3} Br_2 solution (0.66 cm^3, 0.66 mmol) in chloroform. After stirring for 1 h the solution was filtered, and the volume of the filtrate reduced. Addition of methanol precipitated an off-white crystalline product. Yield 0.30 g (0.55 mmol, 63%) (Found: C, 23.95; H, 2.20; Br, 14.60; N, 15.50. Calc. for $C_{11}H_{10}BBrN_6O_2Os$: C, 24.40; H, 1.85; Br, 14.75; N, 15.55%).

(*h*) $[OsBr\{B(pz)_4\}(CO)_2]$ (**11**). A suspension of complex (**5**) (0.52 g, 0.50 mmol) in chloroform (30 cm^3) was treated with a 1 mol dm^{-3} Br_2 solution (0.75 cm^3, 0.75 mmol) in chloroform. After stirring for 1 h the solution was filtered and the volume reduced. Addition of methanol precipitated a cream crystalline product. Yield 0.40 g (0.66 mmol, 66%) (Found: C, 27.00; H, 1.90; Br, 12.50; N, 17.95. Calc. for $C_{14}H_{12}BBrN_8O_2Os$: C, 27.90; H, 2.00; Br, 13.10; N, 18.50%).

Single-crystal Structure Determination for $[\{Ru[HB(pz)_3](CO)_2\}_2]$ (**3**).—A yellow parallelepiped shaped crystal (0.13 × 0.20 × 0.36 mm), grown from methanol solution, was used for data collection. Data were collected on an Enraf-Nonius CAD4 diffractometer using graphite-monochromated Mo-K_α radiation (λ = 0.710 73 Å). The automatic peak-search and reflection-indexing programs, in conjunction with a cell-reduction program, established the crystal system; space-group assignment was made from systematic absences. Cell constants and their estimated standard deviations (e.s.d.s) were obtained by least-squares refinement of the setting angles of 25 reflections. Intensity data were collected by using ω—2θ scans and employing variable speeds to give optimal counting statistics in a minimum time; the scan range was determined as a function of θ to compensate for α_1–α_2 wavelength dispersion. Three standard reflections were chosen and were measured every 60 min of exposure time to check on crystal stability, and every 200 reflections to check the orientation; no significant variations were noted. The data were corrected for Lorentz and polarization effects and for absorption by the method of North *et al.*[27]

Crystal data $C_{22}H_{20}B_2N_{12}O_4Ru_2$, M = 740.25, monoclinic, space group $P2_1/n$, a = 12.439(2), b = 15.380(2), c = 15.571(3) Å, β = 100.85(2)°, U = 2 925.63 Å^3, Z = 4, D_c = 1.68 g cm^{-3}, $F(000)$ = 1 464, μ(Mo-K_α) = 9.68 cm^{-1}.

Data collection. ω Scan angle (0.40 + 0.34 tan θ)°, scan speed 0.21—3.30° min^{-1}, $3 \leqslant \theta \leqslant 27°$, hkl range ±15, +19, +19; 6 840 data measured, 5 914 unique, 5 032 observed [$I \geqslant 2\sigma(I)$]. Number of parameters 446.

Structure solution and refinement. The structure was solved by standard Patterson and Fourier methods and refined by blocked-matrix least-squares calculations using SHELX 76.[28] Anisotropic thermal parameters were used for all non-hydrogen atoms. All hydrogen atoms were located from a difference Fourier map and common isotropic thermal parameters for the pyrazolyl hydrogen atoms belonging to the two independent

Table 3. Fractional co-ordinates ($\times 10^4$, $\times 10^5$ for Ru) for $[\{Ru[HB(pz)_3](CO)_2\}_2]$ (3)

Atom	X/a	Y/b	Z/c	Atom	X/a	Y/b	Z/c
Ru(1)	−8 235(3)	35 316(2)	34 003(2)	Ru(2)	13 368(3)	29 093(2)	33 057(2)
B(1)	−2 979(4)	3 315(4)	1 868(4)	B(2)	2 555(5)	3 100(4)	1 637(4)
C(11)	−603(4)	3 131(3)	4 538(3)	C(21)	1 808(4)	3 334(3)	4 420(3)
C(12)	−163(4)	4 572(3)	3 800(3)	C(22)	916(3)	1 885(3)	3 773(3)
O(11)	−479(3)	2 860(3)	5 238(2)	O(21)	2 131(3)	3 615(3)	5 105(2)
O(12)	184(3)	5 230(2)	4 050(2)	O(22)	744(3)	1 230(2)	4 081(2)
N(111)	−1 734(3)	2 360(2)	2 948(2)	N(211)	1 966(3)	4 072(2)	2 775(3)
N(112)	−2 571(3)	2 416(2)	2 245(2)	N(212)	2 401(3)	3 994(3)	2 037(3)
N(121)	−2 494(3)	4 010(2)	3 349(3)	N(221)	2 948(3)	2 432(2)	3 130(2)
N(122)	−3 273(3)	3 849(2)	2 633(3)	N(222)	3 268(3)	2 545(2)	2 351(2)
N(131)	−1 078(3)	3 944(2)	2 054(2)	N(231)	800(3)	2 481(2)	1 973(2)
N(132)	−2 062(3)	3 789(2)	1 525(3)	N(232)	1 445(3)	2 643(3)	1 376(2)
C(111)	−1 736(4)	1 534(3)	3 234(3)	C(211)	2 189(4)	4 884(3)	3 068(4)
C(112)	−2 560(4)	1 063(3)	2 716(4)	C(212)	2 768(5)	5 327(3)	2 529(5)
C(113)	−3 066(4)	1 633(3)	2 109(3)	C(213)	2 879(4)	4 756(4)	1 894(4)
C(121)	−2 975(5)	4 455(4)	3 907(4)	C(221)	3 756(4)	1 993(3)	3 637(3)
C(122)	−4 066(5)	4 572(4)	3 551(5)	C(222)	4 599(4)	1 828(4)	3 198(4)
C(123)	−4 230(4)	4 193(4)	2 758(5)	C(223)	4 266(4)	2 190(4)	2 397(4)
C(131)	−504(4)	4 418(3)	1 581(3)	C(231)	−56(4)	2 016(3)	1 557(3)
C(132)	−1 104(5)	4 567(4)	754(3)	C(232)	32(5)	1 878(4)	693(3)
C(133)	−2 069(4)	4 154(3)	744(3)	C(233)	983(4)	2 287(4)	608(3)

tridentate ligands refined to 0.050(5) and 0.050(5) Å^2, respectively. Isotropic thermal parameters for H(1) and H(2) were refined independently to values of 0.036(12) and 0.033(11) Å^2, respectively. A weighting scheme $w = 0.6850/\sigma^2(F_o)$ was applied. Final R $\{= (\Sigma\|F_o| - |F_c\|)/\Sigma|F_o|\}$ and R' $\{= [\Sigma w(|F_o| - |F_c|)^2]/\Sigma wF_o^2\}^{\frac{1}{2}}$ values are 0.039 and 0.029, with maximum shift/e.s.d. for positional parameters in the final cycles = 0.06 and maximum residual electron density 0.4 e Å^{-3} (difference map shows no significant features). The final positional parameters for the non-hydrogen atoms are given in Table 3. Atomic scattering factors and anomalous dispersion terms were obtained from ref. 29.

Additional material available from the Cambridge Crystallographic Data Centre comprises H-atom co-ordinates, thermal parameters, and remaining bond lengths and angles.

Acknowledgements

The authors thank Mr. I. Antonowitz from the Structural Chemistry Section of the Division of Processing and Chemical Manufacturing Technology, CSIR, Pretoria, for the variable-temperature n.m.r. experiments.

References

1 G. R. Crooks, B. F. G. Johnson, J. Lewis, I. G. Williams, and G. Gamlen, *J. Chem. Soc. A*, 1969, 2761.
2 A. J. Deeming, N. P. Randle, M. B. Hursthouse, and R. L. Short, *J. Chem. Soc., Dalton Trans.*, 1987, 2473.
3 M. O. Albers, D. C. Liles, E. Singleton, J. E. Stead, and M. M. de V. Steyn, *Organometallics*, 1986, **5**, 1262.
4 S. J. Sherlock, M. Cowie, E. Singleton, and M. M. de V. Steyn, *Organometallics*, 1988, **7**, 1663.
5 E. Singleton, P. H. van Rooyen, and M. M. de V. Steyn, *S. Afr. J. Chem.*, 1989, **42**, 57.
6 E. Singleton, M. O. Albers, and M. M. de V. Steyn, *J. Chem. Soc., Dalton Trans.*, 1989, 2303.
7 M. M. de V. Steyn and E. Singleton, *Acta Crystallogr., Sect. C*, 1988, **44**, 1722.
8 S. J. Sherlock, M. Cowie, E. Singleton, and M. M. de V. Steyn, *J. Organomet. Chem.*, 1989, **361**, 353.
9 R. D. Fisher, A. Vogler, and K. Noack, *J. Organomet. Chem.*, 1967, **7**, 135.
10 J. G. Bullit, F. A. Cotton, and T. J. Marks, *Inorg. Chem.*, 1972, **11**, 671.
11 P. McArdle and A. R. Manning, *J. Chem. Soc. A*, 1970, 2128.
12 P. McArdle and A. R. Manning, *J. Chem. Soc. A*, 1970, 2133.
13 K. Noack, *J. Organomet. Chem.*, 1967, **7**, 151.
14 M. O. Albers, S. F. A. Crosby, D. C. Liles, D. J. Robinson, and E. Singleton, *Organometallics*, 1987, **6**, 2014.
15 A. Shaver, in 'Comprehensive Coordination Chemistry,' ed. G. W. Wilkinson, Pergamon, Oxford, 1987; vol. 2, p. 245.
16 M. I. Bruce, D. N. Sharrocks, and F. G. A. Stone, *J. Organomet. Chem.*, 1971, **31**, 269.
17 A. Eisenstadt, R. Tannenbaum, and A. Efraty, *J. Organomet. Chem.*, 1981, **221**, 317.
18 G. G. Christoph and Y-B. Koh, *J. Am. Chem. Soc.*, 1974, **101**, 1422.
19 B. R. Sutherland and M. Cowie, *Organometallics*, 1984, **3**, 1869.
20 M. Cochivera, T. J. Desmond, G. Ferguson, B. Kaitner, F. J. Lalor, and D. J. O'Sullivan, *Organometallics*, 1982, **1**, 1125.
21 O. S. Mills and J. P. Nice, *J. Organomet. Chem.*, 1967, **9**, 339.
22 K-B. Shlu, M. D. Curtis, and J. C. Huffman, *Organometallics*, 1983, **2**, 936.
23 R. J. Klinger, W. M. Butler, and M. D. Curtis, *J. Am. Chem. Soc.*, 1978, **100**, 5034.
24 J-S. Huang and L. F. Dahl, *J. Organomet. Chem.*, 1983, **243**, 57.
25 E. Singleton, S. Hietkamp, and M. M. de V. Steyn, unpublished work.
26 S. Trofimenko, *Inorg. Synth.*, 1970, **12**, 99.
27 A. C. T. North, D. C. Phillips, and F. S. Matthews, *Acta Crystallogr., Sect. A*, 1968, **24**, 351.
28 G. M. Sheldrick, SHELX 76, Program for Crystal Structure Determination, University of Cambridge, 1976.
29 D. T. Cromer and J. T. Waber, 'International Tables for *X*-Ray Crystallography,' Kynoch Press, Birmingham, 1974, vol. 4, pp. 71—147.

Received 6th March 1990; *Paper* 0/01010C